Topological evolution in the ordered and isotropic phases of a lyotropic system

Doru Constantin
Laboratoire de Physique de l'École Normale Supérieure de Lyon
46 allée d'Italie, 69364 Lyon Cedex 07, France

Contents

Chapter 9 of *Phase Transitions. Applications in Liquid Crystals, Organic Electronic and Optoelectronic Fields*, edited by Vlad Popa-Niță, Research Signpost, Kerala, India, 2006. ISBN 81-308-0062-4. http://www.ressign.com/

1 Introduction

Phase transitions in self-assembling lyotropic mixtures have become a very active field of research in the last twenty years [30]. What sets these phases apart from other soft matter systems (such as colloids or polymers) is that the structure of the surfactant aggregates (the basic "building blocks") changes as a function of the thermodynamical parameters of the system. To put it differently, the energy scales associated with changes in the morphology of the aggregates are of the same order of magnitude as those involved in the change of relative position and orientation of these entities [65]. Furthermore, these typical energies are of the order of the thermal energy, $k_B T \simeq 4\,10^{-21}$ J. As such, both types of processes can occur simultaneously, and must be taken into account if an accurate description is to be obtained.

The behaviour of these systems resulting from a delicate balance between various interactions of similar strength, it should not be surprising that they exhibit a very rich polymorphism. Indeed, both ordered and isotropic phases can be encountered, consisting of different kinds of objects, such as : spherical micelles, long and flexible cylindrical micelles, bilayers (which are 0-dimensional or "point-like", 1-dimensional and 2-dimensional, respectively).

As long as the structure of the aggregates is considered as fixed, they can be treated in the same way as "rigid" colloids [24], as polymer chains [71, 72] or as polymerized membranes [79]. However, if the topology is not constant, its changes have profound effects on the free energy of the phase, first of all by changing the interface energy (see 1.1). Consequently, the topology of the phase is an integral part of a complete description.

Unfortunately, these topology changes (which, in ordered phases, can be seen as "defects" locally breaking the translation symmetry of the phase) can be very difficult to detect by direct methods, such as scattering techniques, because they are not usually ordered, and their structures cannot be resolved in detail. On the other hand, electron microscopy observations should be carefully interpreted, since one can never be sure that the cooling process was fast enough to "freeze" the (sometimes very short-lived) defects.

One can however use alternative approaches : the local curvature of the interfaces can be monitored by NMR (nuclear magnetic resonance) and EPR (electron paramagnetic resonance) techniques, and the transport coefficients of the phase (diffusivity, electrical conductivity etc.) can be measured by appropriate methods. In this case, indirect geometrical information can be obtained by studying the variation of structural properties of the surfactant aggregates (*e.g.* as a function of temperature) starting from a phase of well known structure, that serves as reference. It is especially interesting to perform such measurements on approaching a phase transition, where geometrical changes are bound to occur.

In this review, after a brief overview of fundamental concepts involved in describing the geometrical properties of surfactant aggregates (1.1) and of the experimental system (1.2), I summarize some results obtained recently [19, 20, 21, 18, 17] by such indirect studies on the topology changes in the well-known non-ionic lyotropic system $C_{12}EO_6/H_2O$, by measuring the diffusion constants of tracer molecules in the mesophases (2) and by high-frequency rheology in the isotropic phase (3).

1.1 Geometrical properties

Many excellent descriptions of the geometric properties of surfactant interfaces have been published [27, 54], so in the following we only present a few basic concepts in order to underline the importance of topological changes in lyotropic systems.

The energy of a *fluid* membrane must be invariant under translations and rotations of the whole membrane and homogeneous and isotropic in the plane of the membrane. If we consider the two principal curvatures of the membrane c_1 and c_2, the combinations :

$$\begin{array}{lll} H = & \frac{c_1+c_2}{2} & \text{mean curvature} \\ K = & c_1 c_2 & \text{gaussian curvature} \end{array}$$

are invariant (as the trace and determinant of the curvature tensor, respectively) [66]. To second order in the curvatures, the energy can be written as :

$$E = \int_S \mathrm{d}s \, \left[\sigma + 2\kappa(H - c_0)^2 + \bar{\kappa} K\right] \tag{1}$$

with σ the surface tension, c_0 the spontaneous curvature, κ the bending modulus and $\bar{\kappa}$ the Gaussian modulus of the interface.

Let us now identify the physical counterparts of the elements in the model. In the simplest case, the width of the interface (set by the length of the surfactant molecule) is much smaller than the typical repeat distance in the phase. The relevant interface is either the surfactant monolayer, for microemulsions, or the bilayer, for dilute lamellar or sponge phases. It should be noted that the parameters of the bilayer are easily obtained from those of the monolayer $(\sigma_m, c_{0m}, \kappa_m, \bar{\kappa}_m)$, from simple geometrical considerations [27], yielding :

$$\sigma_b = 2\sigma_m \qquad c_{0b} = 0 \qquad \kappa_b = 2\kappa_m \qquad \bar{\kappa}_b = 2\bar{\kappa}_m + 4\pi\kappa_m c_{0m}\delta \tag{2}$$

where δ is the distance between the midpoints of the two monolayers. Obviously, the spontaneous curvature of the –symmetric– bilayer vanishes (on symmetry grounds) but it is noteworthy that c_{0m} still plays a role : indeed, the monolayers would like to be curved in the same way but, as they are "glued" back to back, decreasing the energy of one side increases the energy of the other. This frustration contributes to the Gaussian modulus $\bar{\kappa}_b$ of the bilayer, increasing its value and thus favouring saddle-like configurations (with $K < 0$).

The last term in the elastic energy (1) can be rewritten using the Gauss-Bonnet theorem [66] :

$$E_{\text{Gauss}} = \bar{\kappa} \int_S \mathrm{d}s \, K = 4\pi\bar{\kappa} \, (1 - g) = 4\pi\bar{\kappa} \, (N_{\text{objects}} - N_{\text{handles}}) \tag{3}$$

where g is the genus (or "number of holes") of the surface; $g = 0$ for a sphere and $g = -1$ for a torus. N_{objects} is the number of disjoint objects formed by the surface and N_{handles} the number of "handles". A fundamental consequence is that, for a system with fixed topology, E_{Gauss} is a constant, so that it does not contribute to the thermodynamics of the

phase. On the other hand, determining the contribution to E_{Gauss} of a topological change, such as creating a new object (*e.g.* breaking a micelle in two) or a handle (*e.g.* creating a hole in a bilayer) is straightforward (+ or $-4\pi\bar{\kappa}$, respectively). Consequently, the role of topological defects in lamellar phases has been extensively studied [26, 52, 28, 22, 37, 11].

1.2 The $C_{12}EO_6/H_2O$ system

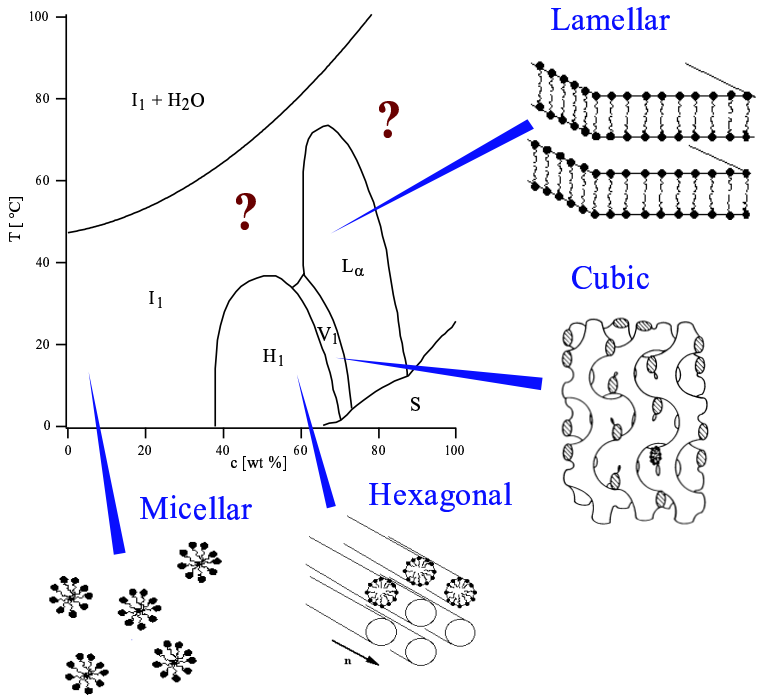

Figure 1: Phase diagram of the $C_{12}EO_6/H_2O$ mixture, redrawn from [50].

The phase diagram of the $C_{12}EO_6/H_2O$ system was determined more than 20 years ago [50]. This binary mixture exhibits three mesophases, namely (on increasing surfactant concentration) the hexagonal H_1, bicontinuous cubic V_1, and lamellar L_α phases. Their characteristics are by now very well established [78]. Due to this rich behaviour and to the reasonable temperature range of the mesophases, they have been extensively studied.However, less attention was given to the isotropic phase (especially in the more concentrated regime) : as in all other surfactant mixtures, it is formed of spherical micelles at very low concentration (see Figure 1), which increase in size with the concentration and temperature, but much less is known about its structure at moderate and high concentration (above about 10%).

2 The mesophases

2.1 Overview

2.1.1 The hexagonal phase

Some measurements aiming to detect the topological changes had already been performed at the hexagonal-isotropic transition, the loss of hexagonal order upon approaching the transition being monitored by NMR and optical birefringence methods [68, 67]. These experiments have shown that a significant fraction of the surfactant molecules form defects near the isotropic liquid, which can be column ends (with spherical caps) or bridges connecting neighbouring columns (see Figure 2). It is clear that the nature of the isotropic liquid will be different depending on the nature of the defects. Indeed, column ends will give rise to isolated micelles whereas bridges should rather announce an isotropic liquid formed of cylinders highly connected to each other and randomly oriented.

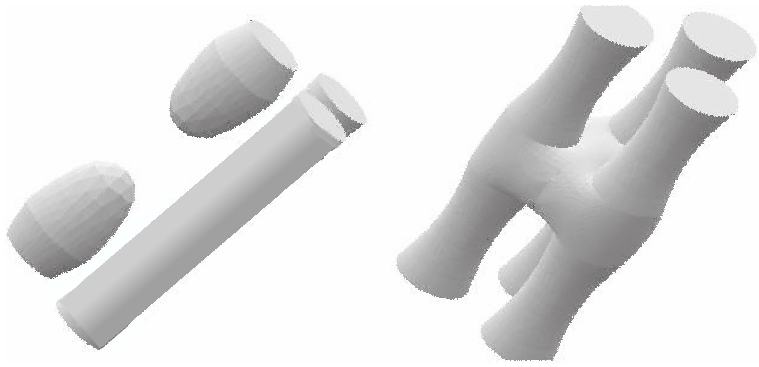

Figure 2: Possible defect structures in the hexagonal phase, close to the transition towards the isotropic phase.

2.1.2 The lamellar phase

Lyotropic lamellar phases contain structural defects that can be point-like or linear (dislocations). Unlike textural defects (*e.g.* focal conics), they are not visible in optical microscopy but can be investigated using techniques such as FFEM (freeze-fracture electron microscopy) [5, 4, 75, 76, 74], SANS (small-angle neutron scattering) [35], spin-labeling EPR [57], birefringence measurements [5, 68], X-ray scattering [61, 16], NMR [70], etc. However, these methods do not give much information about the defect topology.

For instance, in lamellar phases, three elementary point defects are possible : "pores", "necks", and "passages" [34]. Necks connect the non-polar medium (surfactant structure) (Fig. 3a), pores (Fig. 3b) connect the polar medium (water), whereas passages join both media (Fig. 3c). Screw dislocations are also frequent because their energy is low [44]. These defects also connect both media and their core may be filled with the polar or the non-polar medium.

Their study prompted considerable interest in recent years due to their perceived significance in membrane fusion processes (see [81] for a review). Recently, an ordered

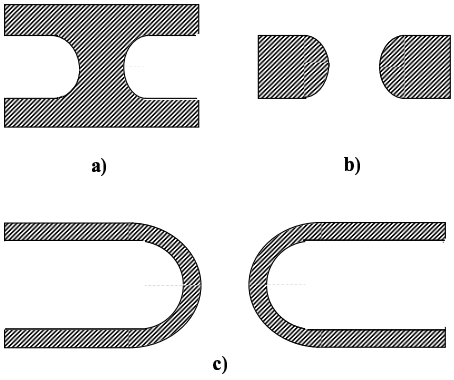

Figure 3: Types of defects in the lamellar phases (from reference [34]) : a – necks, b – pores, c – passages. The surfactant is represented by the cross-hatched texture.

phase of neck-like connections between bilayers was obtained in a phospholipid system [80], allowing a detailed description of the neck structure.

Defects of the "neck" or "pore" types have also been encountered in numerical simulations of lamellar phases of ternary systems close to the transition to the microemulsion phase [29, 36, 11].

In the lamellar phase of $C_{12}EO_6$, spin-labeling EPR measurements [57] have shown the existence of highly curved defects, the density of which abruptly increases a few degrees before melting. Dislocation loops perpendicular to the layers have been observed in FFEM [5, 4] ,but they can only account for a small fraction of the total defect density. It is therefore certain that other defects are also present in the lamellar phase.

2.2 Diffusion coefficients : FRAP measurements

We use the FRAP technique (Fluorescence Recovery After Photobleaching) to determine the diffusion coefficients of fluorescent probes dissolved in the surfactant solution. These probes are either hydrophilic (fluorescein) and hence confined in the aqueous medium or hydrophobic (NBD-dioctylamin) and thus restricted to the medium of the alkyl chains. We can therefore separately probe the topology changes for each medium, which is especially interesting in the case of the lamellar phase.

The experimental setup was originally designed for the study of thin smectic films [9]. The diagram is shown in Figure 2.2 :

We focus the TEM_{00} mode of a multimode Ar^+-ion laser (total power 70 mW) on the sample, bleaching a spot about 40 μm in diameter.The intensity profile of the beam is approximately Gaussian. Typical bleaching times are of the order of 5 seconds.

The evolution of the dark spot is then monitored for one minute using a cooled CCD camera, capturing 30 images. During this time, the initial dark spot extends, due to the diffusion of bleached molecules. The concentration profile is elliptical because of the anisotropic diffusion (Figure 2.2). $D_\perp$ and $D_\parallel$ are obtained from the images by fitting a Gaussian function. The error on the data is estimated from the scatter in values over three to five measurements.

A noteworthy point is that the samples must be oriented in planar anchoring (the

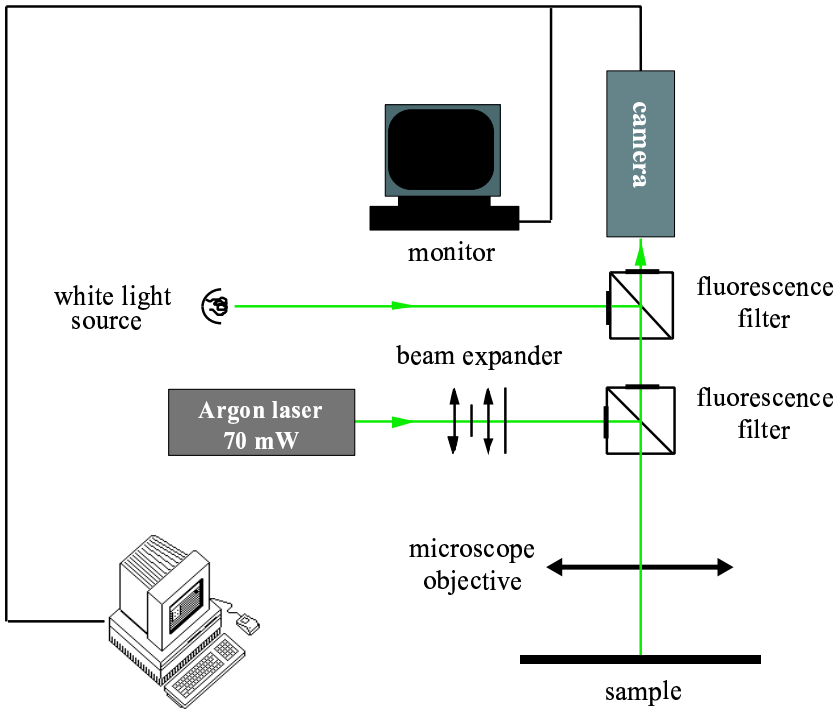

Figure 4: Experimental photobleaching setup.

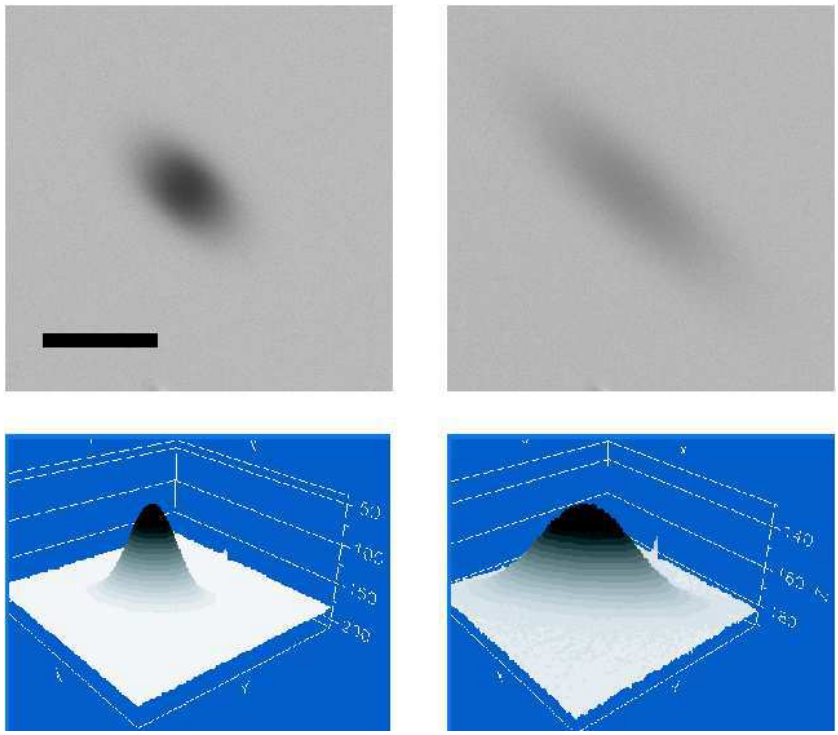

Figure 5: Image of the bleached spot (after background subtraction) and its intensity profile. The images are taken at $t = 0$, immediately after exposure to the laser beam, and $t = 60\,\mathrm{s}$, at the end of the measurement. The bar represents $100\,\mu\mathrm{m}$.

director of the phase contained in the plane of the glass plates) in order to have access to both diffusion coefficients (along and across the surfactant aggregates); this anchoring is easily obtained for the hexagonal phase using glass plates thoroughly cleaned with soap and water, but the lamellar phases usually orients in homeotropic anchoring (with the director perpendicular to the glass plates, in which case only the diffusion coefficient in the plane of the bilayers can be determined). However, we could obtain planar lamellar domains using ITO-covered surfaces (see Figure 6).

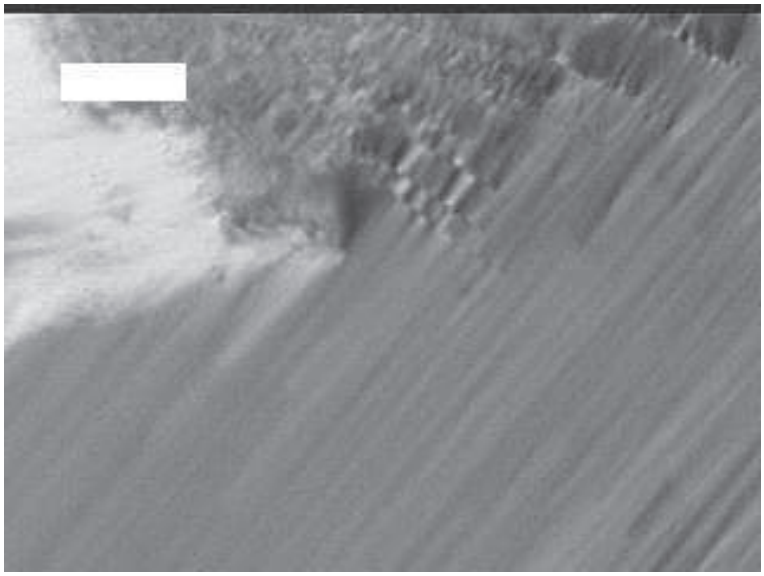

Figure 6: Ordered planar domain of the lamellar phase (at the bottom of the image). The bar represents 200 μm.

Finally, the samples are aligned by slow directional growth in a temperature gradient [56].

2.3 Connections between the surfactant aggregates

2.3.1 Hexagonal phase

In the hexagonal phase, only the hydrophobic probe (NBD dioctylamine) was used, as the aqueous medium is continuous and no significant variations the were expected for the diffusion coefficients of the hydrophilic probe. The results are presented in Figures 7 and 8.

Far from the transition, both $D_{\parallel}$ and $D_{\perp}$ follow Arrhenius laws, with activation energies of 0.35 eV and 0.75 eV, respectively. Over the last five degrees before the transition, $D_{\perp}$ increases rapidly, departing from the low temperature activation law and reaches a value of $4.1\,10^{-12}$ m^2/s at the transition temperature (38.60 °C). The behaviour of D_I (in the isotropic phase), is also well described by an Arrhenius law, with an activation energy of 0.65 eV.

One can relate the pretransitional behaviour of $D_{\perp}$ to the proliferation of structural defects. Clearly, bridges between cylinders (Fig. 2 – b) can provide a passage for the probe

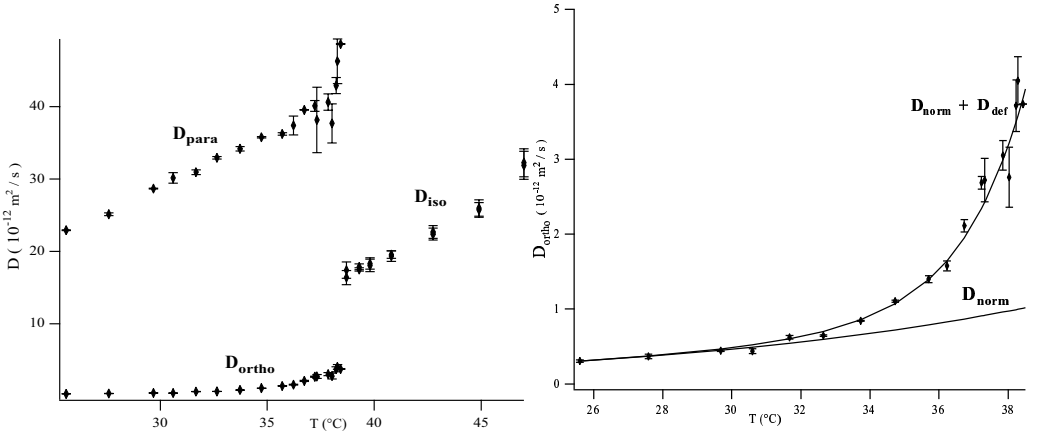

Figure 7: (left) Diffusion coefficients as a function of temperature in the hexagonal and isotropic phases. (right) Diffusion coefficient across the cylinders in the hexagonal phase. $D_{\rm norm}$ is obtained by extrapolating up to the transition temperature the Arrhenius law obtained for $D_\perp$ at low temperature. $D_{\rm def} = D_\perp - D_{\rm norm}$ is fitted to an exponential law (see the text).

molecules. On the other hand, we can exclude the defects of the column end type (Fig. 2 – a), which would lead to a drastic decrease in $D_\parallel$. The structure of the defects was first considered in relation with the study of epitaxial relations between the different ordered phases in the $C_{12}EO_6/H_2O$ system [61, 62]; models for their structure were proposed in terms of Karcher minimal surfaces, connecting three adjacent cylinders [16, 39] (very similar to the representation of bridges in Figure 2 – b). Nevertheless, a detailed description of the defect structure is still lacking; it is likely that a description of the "microemulsion" type, only accounting for the elasticity of the surfactant monolayer (described by the Helfrich Hamiltonian 1) is not appropriate, due to the additional constraints related to the stacking of the alkyl chains (which cannot be treated as a continuous medium, since their conformation is an essential ingredient for describing the elastic properties of the surfactant layer [77]). The solution could thus be very different from a minimal surface. One can however assume that the precise structure of the defects does not affect their role in the diffusion process. Thus, in the minimal model we shall use further, only the topology of the defects is taken into account.

As we are dealing with equilibrium defects, their density is given by a Boltzmann law :

$$n_{\rm def} = n_0 \exp\left(\frac{-E_{\rm def}}{k_B T}\right) \tag{4}$$

where $E_{\rm def}$ is the energy of the defect with respect to a perfectly ordered structure. The considerable increase in defect density close to the transition implies a decrease in energy. The simplest assumption is that of a linear variation :

$$E_{\rm def} = \alpha(T_0 - T) + E_0 \tag{5}$$

Fitting $D_{\rm def}(T)$ with an exponential gives indeed very good results (see Figure 7), yielding a value of $\alpha = 180\, k_B$. The same type of fit applied to $n_{\rm def}(T)$ (equations (4) and (5)) obtained by birefringence and NMR measurements [67] yields a constant $\alpha = 225\, k_B$; One

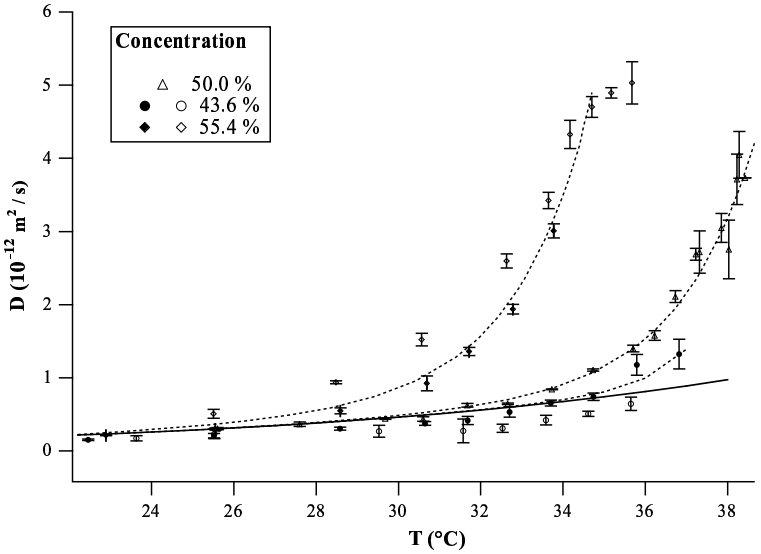

Figure 8: Diffusion coefficient across the cylinders in the hexagonal phase for three concentrations. The solid line represents $D_{\rm norm}$, the value of $D_\perp$ at $c = 50\%$ and low temperature and extrapolated to the transition temperature (see Fig. 7). This baseline seems to be common to the three concentrations. The dotted lines represent the general evolution of $D_\perp$ for the three concentrations.

can consider that $D_{\rm def}$ is proportional to $n_{\rm def}$, showing that the lifetime of the defects is very short[1]. We can thus estimate the average distance between connections at the transition temperature L_0 : $L_0 \simeq 4a \simeq 240$Å, in good agreement with the results of [67], yielding $L_0 \simeq 170$Å. The most important consequence is that the defect density in the hexagonal phase is very large at the transition. The usual image one has of the hexagonal phase as being formed of separate cylinders is no longer correct in these conditions.

One can thus infer that the isotropic phase of the $C_{12}EO_6/H_2O$ mixture above the hexagonal phase is itself highly connected. We further checked this conclusion by measuring the diffusion coefficient across the cubic – isotropic transition. This kind of experiment was already performed by Monduzzi *et al.* [51] for the self-diffusion coefficient of the surfactant in the ionic system CPyCl/NaSal/D_2O. Using NMR techniques, they only observed very small differences between the values of D in the two phases.

Our experimental results for D_C and D_I are shown in Figure 9. The transition temperature is $T_c = 38.25\,^\circ$C. No discontinuity is detected within the experimental precision. One can therefore conclude that, at high surfactant concentration, the topology of the isotropic phase is locally similar to that of the cubic phase (and thus strongly connected), but of course without the long-range order. This result confirms the conclusions drawn from the study of the hexagonal phase.

[1]This conclusion is drawn from numerical simulations showing that $D_\perp$ is proportional to the square of the defect concentration when these are "frozen-in" and linear in the concentration when they are very mobile. See reference [20] for a detailed discussion of this point.

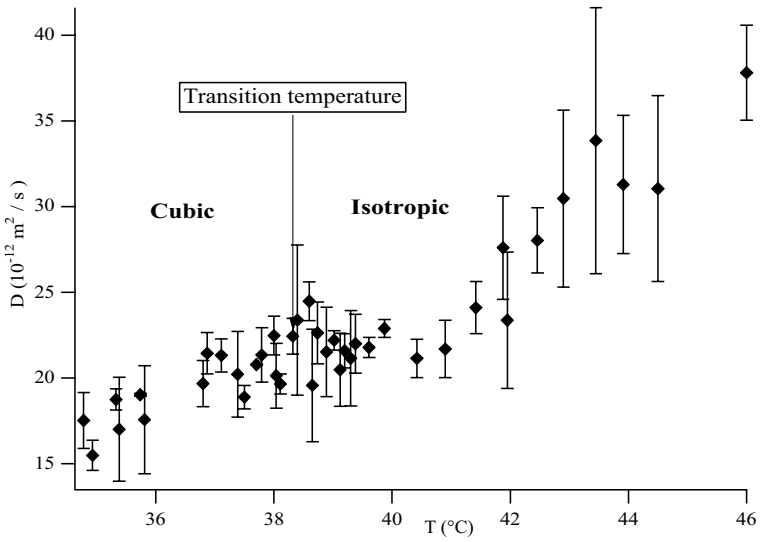

Figure 9: Diffusion coefficients at the cubic – isotropic transition.

2.3.2 Lamellar phase

As for the hexagonal phase, we measured the diffusion coefficients of the hydrophobic probe (NBD dioctylamine), but also that of the hydrophilic molecule (fluorescein) both in the plane of the layers, *i.e.* perpendicular to the director ($D_\perp$; results shown in Fig. 10) and across the layers, parallel to the director ($D_\parallel$, see Fig. 11) [19].

For the hydrophobic probe, $D_\perp$ increases with temperature from 40 10^{-12}m^2/s at 41 °C to 107 10^{-12}m^2/s close to the transition temperature (67.7 °C). No pretransitional effect can be detected (Fig. 10 left).

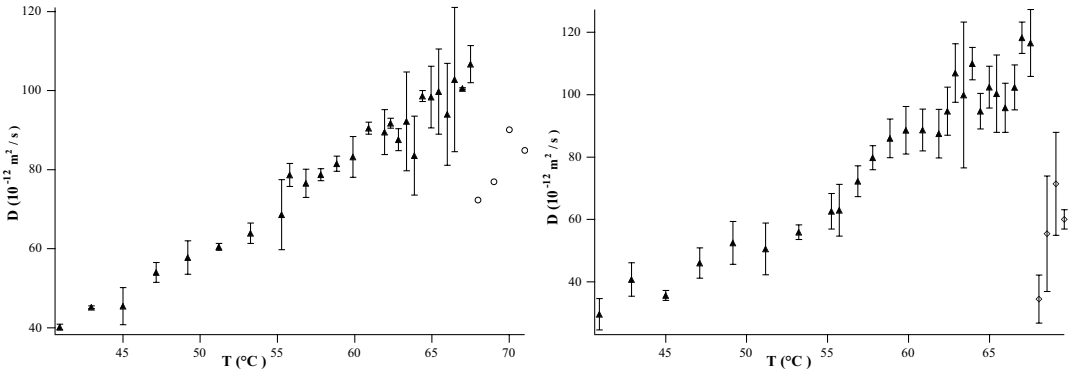

Figure 10: (left) NBD dioctylamine : $D_\perp$ in the lamellar phase (triangles) and D_I in the isotropic phase (open dots). (right) Fluorescein : $D_\perp$ in the lamellar phase (triangles) and D_I in the isotropic phase (diamonds).

The evolution of $D_\parallel$ is completely different : it remains at a value close to 10^{-12}m^2/s up to roughly 55 °C, and then it starts to increase rapidly, reaching 5 10^{-12}m^2/s at the transition (Fig. 11 left). This variation, (denoted by $D_{\rm def} = D_\parallel - D_\parallel^{\rm extr}$, with $D_\parallel^{\rm extr}$ the low-temperature behaviour of $D_\parallel$ extrapolated to the transition temperature), reflects

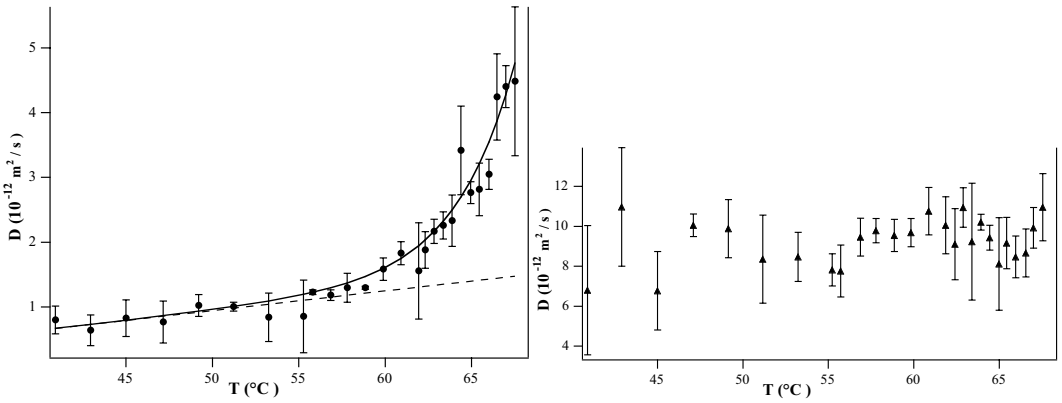

Figure 11: $D_{\|}$ for the two probes. (left) NBD dioctylamine. The dotted line is the extrapolation of the low-temperature behaviour. The solid line is an exponential fit (see the text). (right) Fluorescein. The axes on the right indicate the transition temperature.

the proliferation of new equilibrium defects connecting the surfactant lamellas. Assuming that the defects are point-like, they can be either of the "neck" type, or of the "passage" type. The difference between the two types is that the necks only connect the surfactant, while the passages also connect the aqueous medium. We can discriminate between the two by following the diffusion coefficients of the hydrophilic probe.

$D_{\|}$ of the fluorescein is roughly constant and exhibits no pretransitional effect. Thus, the defects that proliferate at the transition do not increase the connectivity of the aqueous medium, which allows us to conclude that they are of the "neck" type (Fig. 3 – a).

In the following, we shall neglect the contribution of defects other than "necks". We can estimate their density n from the induced diffusion coefficient $D_{\rm def}$:

$$D_{\rm def} \simeq D_{\perp} n \ell^2 \tag{6}$$

up to a numerical prefactor, of order unity. Equation (6) signifies that, as a molecule diffuses into the space occupied by a defect, it crosses to the neighbouring bilayer. From our results, we obtain (immediately before the transition) $n \simeq 0.04\ell^{-2} = 1600\mu\mathrm{m}^{-2}$, meaning that 4 % of molecules participate to the defects. This value is compatible with the increase in the number of defects measured by EPR [57]. It is also likely to participate in the birefringence loss observed in the same temperature range [6].

To evaluate the energy of a defect $E_{\rm def}$, we use the same model as in the hexagonal phase : $n = n_0 \exp(-E_{\rm def}/k_B T)$. For :

$$E_{\rm def} = \alpha(T_0 - T) + E_0 \tag{7}$$

we obtain very good agreement with the experimental data (Figure 11) yielding a constant $\alpha \simeq 100 k_B$. The parameters n_0 and E_0, representing respectively the "highest attainable defect density" and the energy of a defect at the reference temperature T_0 (that we identify to the transition temperature) are not independent : from equation (7), only the $n_0 \exp(-E_0/k_B T)$ product can be obtained. One can nevertheless consider that the size of a defect is of the order of ℓ and, thus, that $n_0 \simeq \ell^{-2}$. This yields $E_0 \simeq 3 k_B T$.

3 The isotropic phase

3.1 Overview

The isotropic phase of the binary system $C_{12}EO_6/H_2O$, as well as those formed by similar non-ionic surfactant molecules, have been studied for more than twenty years; in the beginning, research focused on the structure at low surfactant concentration, especially on the temperature evolution of micellar size and shape. It is now well established that the micelles have a general tendency of increasing in size and becoming anisotropic (cylindrical) with increasing temperature and concentration (see [47] and references therein). It has also been shown that micellar growth strongly depends on the molecular details : it is very important for $C_{12}EO_5$ and $C_{12}EO_6$ but much more modest for $C_{12}EO_8$, which forms short micelles.

When they are not too long, these elongated micelles can be seen as rigid rods, but once they exceed a certain persistence length ℓ_p, they become flexible (estimations for the persistence length of $C_{12}EO_6$ vary from 7 nm [63] to 25 nm [13]). If the micelles are much longer than ℓ_p ("wormlike micelles"), they assume very complex configurations resembling polymers in solution, with the essential difference that the micellar length is not chemically fixed, but rather fluctuates around an equilibrium length depending on the thermodynamical parameters, hence the name of "living polymers". Above an overlap concentration c_c, the micelles begin to touch and become entangled. A quantitative estimate of the curve $c_c(T)$ for the $C_{12}EO_6/H_2O$ system was given in reference [13].

The rheology of entangled polymers is well established [25, 45], and its concepts were recently applied to wormlike micellar systems [15, 32, 31], taking into account the dynamical nature of the micellar length distribution (see [14] for a review). This model was successfully used to describe the rheological behavior of micellar solutions of ionic surfactants [69].

Another interesting property of wormlike micelles is their tendency of interconnecting under certain conditions (concentration, temperature or –in ionic systems– counterion concentration). Such behaviour, first found in ternary systems [58, 55], was subsequently observed in a very wide range of binary mixtures of single-tail non-ionic [3, 41, 42, 40, 48, 10] or double-tail zwitterionic [73, 7] surfactants, as well as in pseudo-binary systems (ionic surfactant + brine) [51, 8, 43, 53, 33, 1, 2, 60].

Structurally, connected and entangled systems only differ on a very small scale, which makes them difficult to tell apart using static techniques. Furthermore, the microscopic structure of the connections is far from being elucidated (see [49] and references therein). Indirect techniques must then be employed; for instance, the minimum in surfactant self-diffusion coefficient as a function of the concentration appearing in a wide variety of systems was often explained by the appearance of connections [41]. However, it was shown [69] that this behavior could also originate in the competition between two different mechanisms : diffusion of the micelle itself and diffusion of the surfactant molecule on the micelle.

On the other hand, connections can have a dramatic effect on the *dynamical* properties of wormlike micellar systems. Contrary to connected polymer systems, where the reticulation points (permanent chemical cross-links) slow down the dynamics, connections

between entangled micelles can actually facilitate relaxation and render the system more fluid. This aspect prompted a systematic study of the connectivity in micellar solutions : several experiments [8, 43, 64] showed that, in ionic surfactant systems, the viscosity decreases on increasing the salt concentration. They were followed by theoretical works on the conditions of connection formation [23] and their influence on the dynamics of the phase [46]. The theory was then employed to qualitatively characterize the appearance of connections [53, 33, 2]. Briefly, branching points allow the surfactant to "flow" more easily across the micellar network, thus increasing the curvilinear diffusion constant of a micelle D_c. As the terminal relaxation time in entangled systems is the reptation time $\tau_R = L^2/D_c$, this amounts (from the dynamical point of view) to replacing the average length of a micelle by the average distance between branching points along a micelle [14]. When the latter becomes of the order of the entanglement length, the network is termed "saturated" [23]; in this case, the concept of reptation is no longer valid and other relaxation mechanisms, such as those related to the local order, can become dominant [21].

3.2 Theoretical considerations

The main relaxation process in entangled polymer solutions is reptation, by which the chain gradually disengages from its initial deformed environment ("tube") and adopts a stress-free configuration. The typical reptation time is given by : $\tau_{rep} \simeq L^2/D_c$, with L the chain length and D_c the curvilinear diffusion constant of the micelle in its tube [45], and the shear modulus exhibits exponential decay : $G(t) \sim \exp(-t/\tau_{rep})$. In the case of wormlike micellar systems, the length distribution $c(L)$ must be taken into account and the resulting relaxation is highly non-exponential [15] :

$$G(t) \sim \exp\left[-\left(\frac{t}{\tau_{rep}}\right)^{1/4}\right], \tag{8}$$

where τ_{rep} is now given by :

$$\tau_{rep} = \frac{L_m^2}{D_c}, \tag{9}$$

with L_m the micellar length averaged over $c(L)$.

Another distinctive feature of wormlike micelles is that they can break up and reform, with a typical time τ_{br}. For $\tau_{br} \gg \tau_{rep}$, the dynamical response (8) is not affected; in the opposite limit, $\tau_{br} \ll \tau_{rep}$, $G(t)$ approaches a single exponential [15], with relaxation time $\tau \simeq \sqrt{\tau_{br}\tau_{rep}}$. Besides reptation, which is a process involving the entire chain, additional (local) relaxation modes are present at higher frequency, given by "breathing" (tube length fluctuations) and Rouse dynamics [32, 31].

As discussed in reference [21], when the system exhibits local order (induced by the micelle-micelle interaction) with a range d, one can only observe elastic behavior by probing the system on scales smaller than this correlation distance. The time τ needed to relax the stress can then be estimated as :

$$\tau \sim \frac{d^2}{6D}, \tag{10}$$

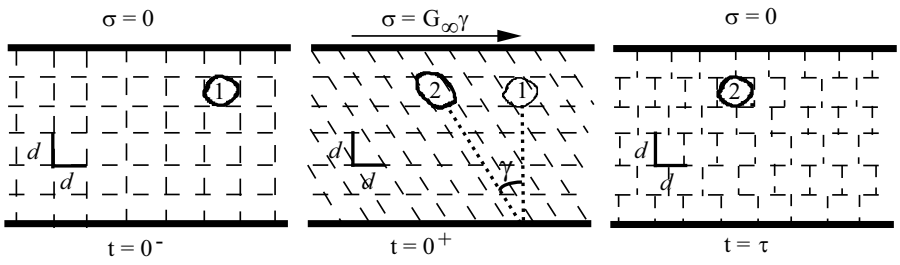

Figure 12: Schematic representation of shear in a material consisting of units of typical size d. One such unit (thick line contour) has been displaced between points 1 and 2. The instantaneous elastic stress is $\sigma = G_\infty \gamma$; it relaxes over a typical time τ given by equation (10).

where D is the collective diffusion constant. A pictorial representation is given in Figure 12 : consider a material with short-range order confined between two plates. The system can be seen as consisting of elasticity-endowed units of typical size d, the correlation distance. After applying an instantaneous shear γ by moving the upper plate to the left, one such unit (represented in thick line) has been advected from point 1 to point 2. At time $t = 0^+$ after the deformation, the stress on the upper plate is $\sigma = G_\infty \gamma$, with G_∞ the instantaneous ("infinite" frequency) shear modulus of the elastic material. Since there is no long-range restoring force, once the particles equilibrate their internal configuration (over a distance d), the elastic stress is completely relaxed; thus, after a time τ given by eq. 10, $\sigma = 0$.

When the system is not completely connected, both previously described processes are relevant so, in the simplest approximation, we can assume that the shear modulus is a sum of two mechanisms, one related to polymer-like dynamics and the other given by order relaxation, each one with a characteristic time scale. Thus, in the first approximation we expect a bimodal relaxation of the form $G(t) = G_{\infty 1} \exp(-t/\tau_1) + G_{\infty 2} \exp(-t/\tau_2)$ or, in the frequency domain :

$$G^*(\omega) = G' + iG'' = \frac{i\omega\eta_1}{1 + i\omega\tau_1} + \frac{i\omega\eta_2}{1 + i\omega\tau_2} \tag{11}$$

where τ_1 and τ_2 are the respective relaxation times, while G' and G'' are the storage and loss moduli, describing elasticity and dissipation, respectively. We express the complex shear modulus $G^*(\omega)$ as a function of the terminal viscosities η_1 and η_2 which can be more reliably determined from the low-frequency data than the plateau moduli $G_{\infty i} = \eta_i/\tau_i$, $i = 1, 2$. For definiteness, subscript '1' will denote the slower relaxation mechanism (*i.e.* $\tau_1 > \tau_2$).

3.3 High-frequency rheology

Before discussing the frequency dependence of the viscoelastic parameters, let us present the results of low-frequency viscosity η_0 measurements in $C_{12}EO_6/H_2O$ and in the related system $C_{12}EO_8/D_2O$, where the micelles are known to remain rather small [47]. If the complex shear modulus is of the form 11, then $\eta_0 = \eta_1 + \eta_2$. For $C_{12}EO_6/H_2O$, we also plot the results of Strey [74] (full and dotted lines) obtained by a different method. The two sets of data agree quite well.

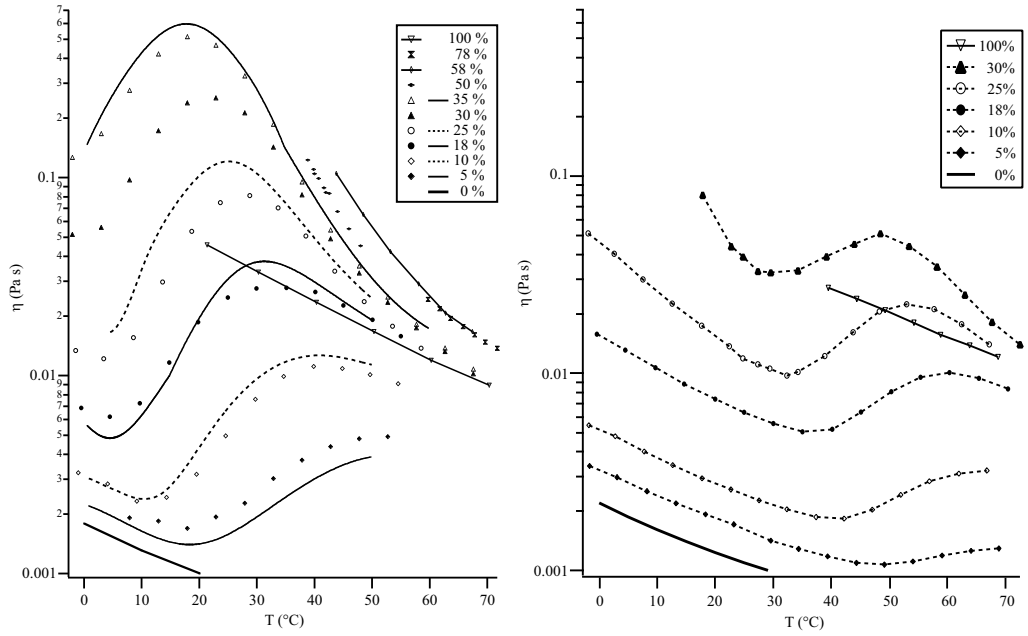

Figure 13: Left : Low frequency viscosity at different concentrations and temperatures in the isotropic phase of the $C_{12}EO_6/H_2O$ mixture (various symbols) compared to the results of Strey [74] (full and dotted lines). Right : Low frequency viscosity in the isotropic phase of the $C_{12}EO_8/D_2O$ mixture.

Clearly, the behaviour of η_0 is quite different in the two systems; in particular, in $C_{12}EO_6/H_2O$ it exhibits a strong increase in temperature and then (at high concentration, at least) decreases after a maximum. Using high-frequency rheology allows us to separate the different mechanisms contributing to η_0.

We start the discussion with the study of the isotropic phase of $C_{12}EO_6/H_2O$, above the hexagonal phase reference ($c = 50\%$, $T > 40\,^{\circ}C$) [21]. A representative spectrum is shown in Figure 14. A single relaxation mode is detected, with a characteristic time of about 1 μs. In accordance with the theoretical discussion in the previous section, we assign this time to the relaxation of the local micellar order evidenced by X-ray scattering [20]. The absence of any low-frequency mode confirms our conclusion that the isotropic phase is highly connected (see 2.3.1).

For lower concentrations ($c = 35$ and 30%), the curves are well fitted with the sum of two Maxwell models (11). In figure 15 we show the data for $c = 35\%$: G' and G'' as a function of ω for three temperature points (8, 23 and 33 °C) and the value of the fit parameters in equation (11).

On the other hand, there is no sign of the slow relaxation mode for the $C_{12}EO_8/D_2O$ system; for $c \leq 25\%$ the system is purely viscous in the investigated frequency range (there is no detectable storage modulus), and the values for the low-frequency viscosity are given in figure 13 (right).

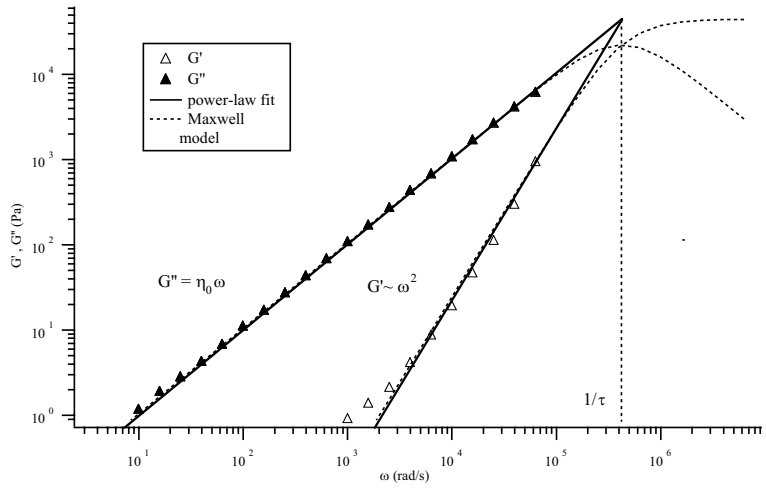

Figure 14: Typical data fit at $c = 50\%$ (here, for $T = 40\,^\circ$C) : solid line, power-law fit ($G' \propto \omega^2$ et $G'' = \eta_0\omega$). The curves cross at a frequency $\omega = 1/\tau$, with τ the terminal relaxation time. Dotted line, fit with a model Maxwell with parameters η_0 and τ.

3.4 Interpretation

Let us now quantitatively discuss the fast relaxation time (see Equation 10). At $c = 50\%$, $d \sim 25 - 40\,$nm and $D \sim 1.5\,10^{-10}\,\mathrm{m}^2/\mathrm{s}$, leading to a relaxation time $\tau \sim 1\,\mu$s. D decreases at lower concentration [12], as well as the correlation range [82], but we have no quantitative estimate for the latter. For the plateau modulus G_∞ one can take –in a first approximation– the shear modulus of the hexagonal phase, because at high frequency the structure is probed on scales smaller than the correlation length, where it is locally organized. Its value, $G_\infty \sim 5\,10^4\,\mathrm{Pa}^2$ is in good agreement with the experimental results.

At lower concentration, both the relaxation time τ_2 (in the μs range) and the plateau modulus $G_{\infty 2} \sim 2\,10^4\,$Pa at $30 - 35\%$ – figure 15) are coherent with the values obtained for $c = 50\%$. This mechanism is also detected in the $C_{12}EO_8/D_2O$ system at $c = 30\%$; the corresponding viscosity is presented in figure 13 (right) and the relaxation time and plateau modulus (only detectable by our technique between about $40 - 55\,^\circ$C) are given in figure 16.

As to the slow relaxation mechanism, it is only present in the $C_{12}EO_6/H_2O$ system, with longer micelles, and it does not appear in the $C_{12}EO_8/D_2O$ solution, where the micelles are shorter. We can therefore consider that it is due to the entangled network relaxing by micellar reptation. The relaxation time τ_1 first increases with temperature, goes through a maximum and subsequently decreases. The viscosity $\eta_1 = G_{\infty 1}\tau_1$ has a similar evolution. The temperature position of the maximum goes from $18\,^\circ$C at $c = 35\%$ to $35\,^\circ$C at $c = 18\%$. As discussed in the theoretical section, this variation can be understood as an increase in micellar size, followed by the appearance of connections. This variation is coherent with the fact that the curvature of the aggregates diminishes with increasing temperature (due to the decreasing hydration of the nonionic polar groups [59, 38]), favouring low-curvature junctions over high-curvature end-caps. τ_1 takes values

[2]Pawel Pieranski, private communication.

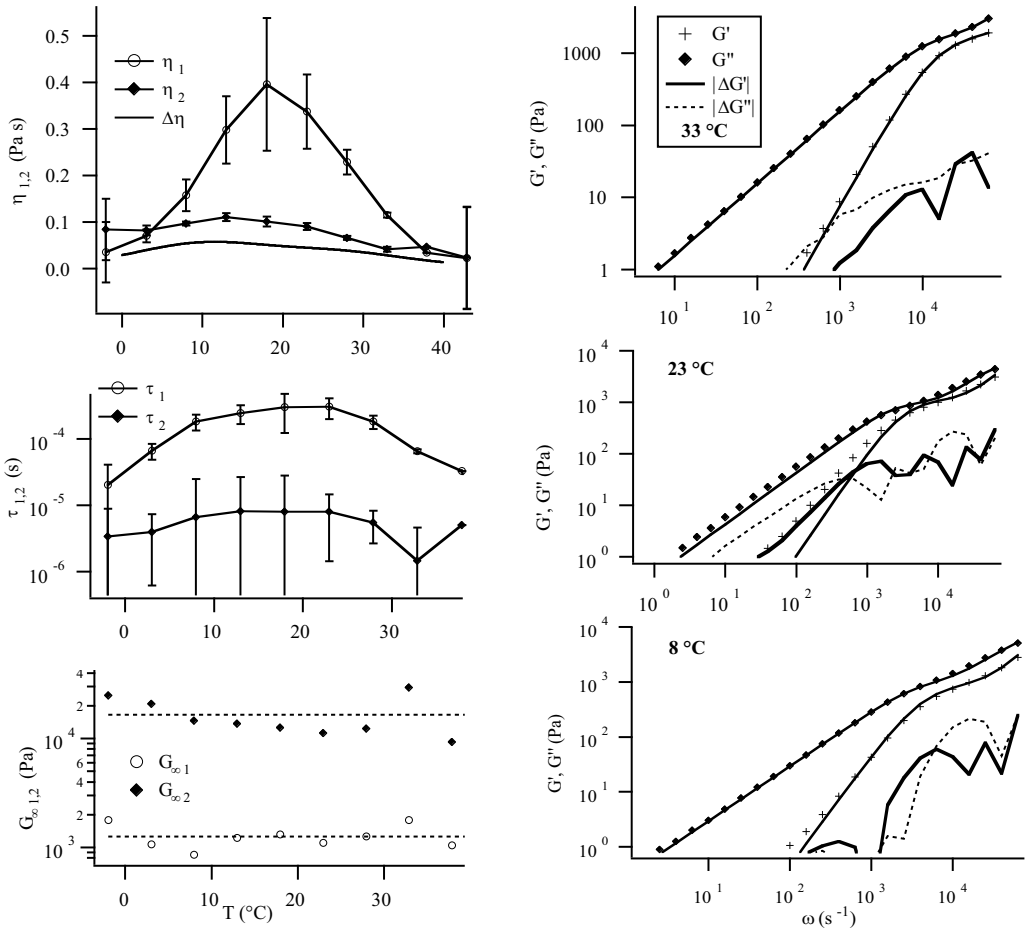

Figure 15: Rheology data for the $C_{12}EO_6/H_2O$ system at $c = 35\%$. Left : Value of the fit parameters in equation (11), as well as $G_{\infty i} = \eta_i/\tau_i$. Right : The value of G' and G'' as a function of ω and the corresponding fit with two Maxwell models (for 33 °C, 23 °C and 8 °C).

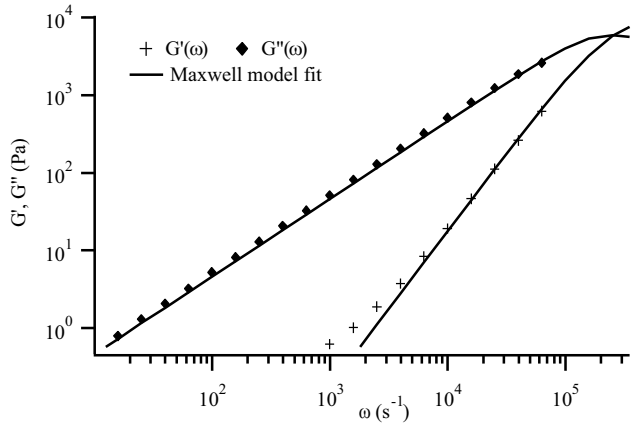

Figure 16: Rheology results for the $C_{12}EO_8/D_2O$ mixture at $c = 30\%$: Maxwell model fit at $T = 48.5\,°C$ a) relaxation time τ b) and plateau modulus G_∞ c) as a function of temperature.

around 10^{-4} s (figure 15), much smaller than the usual reptation times in wormlike micellar systems [1, 53, 43]; the difference could be a sign that the entangled micelles become connected before they reach a sizeable length.

We would like to point out that solutions of lecithin/ H_2O/n-decane exhibit a similar bimodal relaxation spectrum (as recently shown by Schipunov and Hoffmann [73]) where the low-frequency mechanism seems to disappear upon heating (see their figure 18). As these systems are very viscous and the entire relaxation spectrum is accessible to conventional rheometers, a systematic investigation of their behavior in concentration and temperature could yield interesting information.

4 Conclusion

We highlighted the utility of indirect methods for the study of structural changes in lyotropic systems by measuring the diffusion coefficients of fluorescent probes (along and across the director) in the ordered phases of a nonionic lyotropic system.

The temperature evolution of these coefficients shows that, on approaching the transition towards the isotropic phase, the structure formed by the surfactant becomes more and more connected (the probe molecules pass more easily from a cylinder to the next in the hexagonal phase and between neighbouring bilayers in the lamellar phase). We quantitatively characterized these defects as to their density and, in the hexagonal phase, we could show that their lifetime is very short (on the order of the microsecond). Thus, they are equilibrium defects, and their density becomes important close to the transition.

This topological evolution provides insight into the microstructure of the isotropic phase above the ordered phases (at high surfactant concentration), which is strongly connected, in contrast with the typically considered models of the "giant micelles" type.

This investigation was continued by another indirect method, dealing this time with the dynamical properties of the isotropic phase, studied by high-frequency rheology. In the concentrated regime, the structure exhibits an extremely short terminal relaxation time (in the microseconds), that we attributed to the short-range hexagonal order detected by X-ray scattering experiments. The lack of a lower-frequency relaxation can be explained by the fact that, in a strongly connected system, the "polymer"-type modes(dominant if the micelles are only entangled) disappear; such an interpretation is in agreement with the conclusions drawn from the experiments on diffusion coefficients.

Nevertheless, such slow modes are present at intermediate surfactant concentrations, where the isotropic phase can be foud at lower temperatures. Their amplitude evolves with temperature in a non-monotonous manner : first it increases and then, after a maximum, it decreases and finally disappears. This feature can be explained by a topological transition starting (at low temperature) with small spherical micelles, which grow in size and become elongated (leading to an increase in viscosity) until a point where they start to form connections (which, being mobile, allow the surfactant to flow through the structure and render the phase more fluid). Finally, the phase becomes totally connected and the slow mode disappears completely. This is the only stage that can be observed at high concentration, where the isotropic phase is limited at lower temperature by the mesophases.

We hope this was convincing enough evidence that the study of such morphological changes without thermodynamical transition is quite interesting; on the one hand because the properties of the system can change substantially even though it remains within the same phase and, on the other, because such changes often "announce" the transition towards a different phase and can therefore yield important information on its structure.

References

[1] A. Aït Ali and R. Makhloufi. Linear and nonlinear rheology of an aqueous concentrated system of cethyltrimethylammonium chloride and sodium salicylate. *Phys. Rev. E*, 56(4):4474–4478, 1997.

[2] A. Aït Ali and R. Makhloufi. Effect of organic salts on micellar growth and structure studied by rheology. *Colloid. Polym. Sci.*, 277:270–275, 1999.

[3] E. Alami, N. Kamenka, A. Raharimihamina, and R. Zana. Investigation on the microstructures in mixtures of water with the nonionic surfactants C_8E_5 , $C_{10}E_6$, and $C_{10}E_8$ in the whole range of composition. *J. Coll. Interf. Sci.*, 158:342–350, 1993.

[4] M. Allain. Possible defect–mediated phase transition in a lyotropic liquid crystal. Electron microscopy observations. *Europhys. Lett.*, 2(8):597–602, 1986.

[5] M. Allain and J.-M. di Meglio. Highly curved defects in lyotropic lamellar phases. *Mol. Cryst. Liq. Cryst.*, 124(1-4):115–124, 1985.

[6] M. Allain, P. Oswald, and J.-M. di Meglio. Structural defects and phase transition in a lyotropic system : Optical birefringence and order parameter measurements. *Mol. Cryst. Liq. Cryst.*, 162(B):161–169, 1988.

[7] L. Ambrosone, R. Angelico, A. Ceglie, U. Olsson, and G. Palazzo. Molecular diffusion in a living network. *Langmuir*, 17(22):6822–6830, 2001.

[8] J. Appell, G. Porte, A. Khatory, F. Kern, and S. J. Candau. Static and dynamic properties of a network of wormlike surfactant micelles (cetylpyridinium chlorate in sodium chlorate brine). *J. Phys. II (France)*, 2(5):1045–1052, 1992.

[9] J. Bechhoefer, J.-C. Géminard, L. Bocquet, and P. Oswald. Experiments on tracer diffusion in thin free–standing liquid crystal films. *Phys. Rev. Lett.*, 79(24):4922–4925, 1997.

[10] A. Bernheim-Groswasser, E. Wachtel, and Y. Talmon. Micellar growth, network formation, and criticality in aqueous solutions of the nonionic surfactant $C_{12}E_5$. *Langmuir*, 16(9):4131–4140, 2000.

[11] T. Biben and K. Helal. Stress induced topological fluctuations in confined lamellar systems. *Molecular Physics*, 101(11):16831696, 2003.

[12] W. Brown and R. Rymdén. Static and dynamical properties of a nonionic surfactant ($C_{12}E_6$) in aqueous solution. *J. Phys. Chem.*, 91(13):3565–3571, 1987.

[13] T. R. Carale and D. Blankschtein. Theoretical and experimental determinations of the crossover from dilute to semidilute regimes of micellar solutions. *J. Phys. Chem.*, 96(1):459–467, 1992.

[14] M. E. Cates. Flow behaviour of entangled surfactant micelles. *J. Phys. Cond. Matt.*, 8:9167–9176, 1996.

[15] M. E. Cates and S. J. Candau. Statics and dynamics of worm-like surfactant micelles. *J. Phys. Cond. Matt.*, 2:6869–6892, 1990.

[16] M. Clerc, A.-M. Levelut, and J.-F. Sadoc. Transitions between mesophases involving cubic phases in the surfactant–water systems. Epitaxial relations and their consequences in a geometrical framework. *J. Phys. II (France)*, 1(10):1263–1276, 1991.

[17] D. Constantin. *Equilibrium defects in the ordered phases and structure of the isotropic liquid of a lyotropic mixture of nonionic surfactant (in French).* PhD thesis, École Normale Supérieure de Lyon, 2002.

[18] D. Constantin, Éric Freyssingeas, J.-F. Palierne, and P. Oswald. Structural transition in the isotropic phase of the $C_{12}EO_6/H_2O$ lyotropic mixture: A rheological investigation. *Langmuir*, 19(7):2554–2559, 2003.

[19] D. Constantin and P. Oswald. Diffusion coefficients in a lamellar lyotropic phase: Evidence for defects connecting the surfactant structure. *Phys. Rev. Lett.*, 85(20):4297–4300, 2000.

[20] D. Constantin, P. Oswald, M. Impéror-Clerc, P. Davidson, and P. Sotta. Connectivity of the hexagonal, cubic and isotropic phases of the $C_{12}EO_6/H_2O$ lyotropic mixture investigated by tracer diffusion and X-ray scattering. *J. Phys. Chem. B*, 105(3):668–673, 2001.

[21] D. Constantin, J.-F. Palierne, Éric Freyssingeas, and P. Oswald. High-frequency rheological behaviour of a multiconnected lyotropic phase. *Europhys. Lett.*, 58(2):236–242, 2002.

[22] R. de Vries. Passages in lamellar phases of highly charged fluid membranes. *J. Chem. Phys.*, 103(15):6740–6748, 1995.

[23] T. J. Drye and M. E. Cates. Living networks : The role of cross-links in entangled surfactant solutions. *J. Chem. Phys.*, 96(2):1367–1374, 1992.

[24] D. F. Evans and H. Wennerström. *The Colloidal Domain. Where Physics, Chemistry, Biology and Technology Meet.* Wiley VCH, New York, 2 edition, 1999.

[25] J. D. Ferry. *Viscoelastic Properties of Polymers.* John Wiley and Sons, New York, 3 edition, 1980.

[26] L. Golubović. Passages and droplets in lamellar fluid membranes. *Phys. Rev. E*, 50(4):R2419–R2422, 1994.

[27] G. Gompper. Statistical mechanics of membranes. In J. K. G. Dhont, G. Gompper, and D. Richter, editors, *Soft Matter : Complex Materials on Mesoscopic Scales*. Forschungszentrum Jülich, Jülich, 2002.

[28] G. Gompper and G. Goos. Fluctuations and phase behavior of passages in a stack of fluid membranes. *J. Phys. II (France)*, 5(4):621–634, 1995.

[29] G. Gompper and D. M. Kroll. Phase diagram of fluid vesicles. *Phys. Rev. Lett.*, 73(15):2139–2142, 1994.

[30] G. Gompper and M. Schick. Self-assembling amphiphilic systems. volume 16 of *Phase transitions and critical phenomena*. Academic Press, London, 1994.

[31] R. Granek. Dip in $G''(\omega)$ of polymer melts and semidilute solutions. *Langmuir*, 10(5):1627–1629, 1994.

[32] R. Granek and M. E. Cates. Stress relaxation in living polymers : Results from a Poisson renewal model. *J. Chem. Phys.*, 96(6):4758–4767, 1992.

[33] P. A. Hassan, S. J. Candau, F. Kern, and C. Manohar. Rheology of wormlike micelles with varying hydrophobicity of the counterion. *Langmuir*, 14(21):6025–6029, 1998.

[34] W. Helfrich. Amphiphilic mesophases made of defects. In R. Balian, M. Kléman, and J.-P. Poirier, editors, *Physics of Defects*. North–Holland, Amsterdam, 1980.

[35] M. Holmes, A. Smith, and M. Leaver. A small angle neutron scattering study of the lamellar phase of caesium pentadecafluorooctanoate(CsPFO)/ 1H-1H-perfluoroheptan-1-ol/^2H_2O. *J. Phys. II (France)*, 3(9):1357–1370, 1993.

[36] R. Hołyst and W. T. Góźdź. Fluctuating Euler characteristics, topological disorder line, and passages in the lamellar phase. *J. Chem. Phys.*, 106(11):4773–4780, 1997.

[37] R. Hołyst and B. Przybylski. Topological Lifshitz line, off-specular scattering, and mesoporous materials. *Phys. Rev. Lett.*, 85(1):130–133, 2000.

[38] J. N. Israelachvili. *Intermolecular & Surface Forces*. Academic Press, London, 2 edition, 1992.

[39] H. Karcher. The triply periodic minimal surfaces of Alan Schoen and their mean curvature companions. *Manuscr. Math.*, 64:291–357, 1989.

[40] T. Kato. Surfactant self-diffusion and networks of wormlike micelles in concentrated solutions of nonionic surfactants. *Progr. Colloid Polym. Sci.*, 100:15–18, 1996.

[41] T. Kato, T. Terao, and T. Seimiya. Intermicellar migration of surfactant molecules in entangled micellar solutions. *Langmuir*, 10(12):4468–4474, 1994.

[42] T. Kato, N. Toguchi, T. Terao, and T. Seimiya. Structure of networks formed in concentrated solutions of nonionic surfactant studied by the pulsed-gradient spin-echo method. *Langmuir*, 11(12):4661–4664, 1995.

[43] A. Khatory, F. Kern, F. Lequeux, J. Appell, G. Porte, N. Morie, A. Ott, and W. Urbach. Entangled versus multiconnected network of wormlike micelles. *Langmuir*, 9(4):933–939, 1993.

[44] M. Kléman. *Points, Lines and Walls: in Liquid Crystals, Magnetic Systems, and Various Disordered Media*. John Wiley, New York, 1983.

[45] R. G. Larson. *The Structure and Rheology of Complex Fluids*. Topics in Chemical Engineering. Oxford University Press, New York • Oxford, 1999.

[46] F. Lequeux. Reptation of connected wormlike micelles. *Europhys. Lett.*, 19(8):675–681, 1992.

[47] B. Lindman and H. Wennerström. Nonionic micelles grow with increasing temperature. *J. Phys. Chem.*, 95(15):6053–6054, 1991.

[48] F. Mallamace and D. Lombardo. Light-scattering studies on water–nonionic-amphiphile solutions. *Phys. Rev. E*, 51(3):2341–2348, 1995.

[49] S. May, Y. Bohbot, and A. Ben-Shaul. Molecular theory of bending elasticity and branching of cylindrical micelles. *J. Phys. Chem. B*, 101(43):8648–8657, 1997.

[50] D. J. Mitchell, G. J. Tiddy, L. Waring, T. Bostock, and M. P. McDonald. Phase behaviour of polyoxyethylene surfactants with water. *J. Chem. Soc. Faraday Trans. I*, 79:975–1000, 1983.

[51] M. Monduzzi, U. Olsson, and O. Söderman. Bicontinuous "micellar" solutions. *Langmuir*, 9(11):2914–2920, 1993.

[52] D. C. Morse. Topological instabilities and phase behavior of fluid membranes. *Phys. Rev. E*, 50(4):R2423–R2426, 1994.

[53] J. Narayanan, C. Manohar, F. Kern, F. Lequeux, and S. J. Candau. Linear viscoelasticity of wormlike micellar solutions found in the vicinity of a vesicle-micelle transition. *Langmuir*, 13(20):5235–5243, 1997.

[54] D. Nelson, S. Weinberg, and T. Piran, editors. *Statistical Mechanics of Membranes and Surfaces*. World Scientific, Singapore, 2 edition, 2004.

[55] B. W. Ninham, I. S. Barnes, S. T. Hyde, P. J. Derian, and T. N. Zemb. Random connected cylinders : A new structure in three-component microemulsions. *Europhys. Lett.*, 4(5):561–568, 1987.

[56] P. Oswald, M. Moulin, P. Metz, J.-C. Géminard, P. Sotta, and L. Sallen. An improved directional growth apparatus for liquid crystals : applications to thermotropic and lyotropic systems. *J. Phys. III (France)*, 3(9):1891–1907, 1993.

[57] L. Paz, J. M. Di Meglio, M. Dvolaitzky, R. Ober, and C. Taupin. Highly curved defects in lyotropic (nonionic) lamellar phases. origin and role in hydration process. *J. Phys. Chem.*, 88(16):3415–3418, 1984.

[58] G. Porte, R. Gomati, O. El Haitamy, J. Appell, and J. Marignan. Morphological transformations of the primary surfactant structures in brine-rich mixtures of ternary systems (surfactant/alcohol/brine). *J. Phys. Chem.*, 90(22):5746–5751, 1986.

[59] S. Puvvada and D. Blankschtein. Molecular–thermodynamic approach to predict micellization, phase behaviour and phase separation of micellar solutions. I. Application to nonionic surfactants. *J. Chem. Phys.*, 92(6):3710–3724, 1990.

[60] S. R. Raghavan, H. Edlund, and E. W. Kaler. Cloud-point phenomena in wormlike systems containing cationic surfactant and salt. *Langmuir*, 18(4):1056–1064, 2002.

[61] Y. Rançon and J. Charvolin. Epitaxial relationships during phase transformations in a lyotropic liquid crystal. *J. Phys. Chem.*, 92(9):2646–2651, 1988.

[62] Y. Rançon and J. Charvolin. Fluctuations and phase transformations in a lyotropic liquid crystal. *J. Phys. Chem.*, 92(22):6339–6344, 1988.

[63] J. C. Ravey. Lower consolute curve related to micellar structure of nonionic surfactants. *J. Coll. Interface Sci.*, 94(1):289–291, 1983.

[64] H. Rehage and H. Hoffmann. Rheological properties of viscoelastic surfactant systems. *J. Phys. Chem.*, 92(16):4712–4719, 1988.

[65] S. Safran. *Statistical Thermodynamics of Surfaces, Interfaces, and Membranes*. Addison-Wesley, Reading, Mass, 1994.

[66] S. Safran. Curvature elasticity of thin films. *Adv. Phys.*, 48(4):395–448, 1999.

[67] L. Sallen. *Elasticity and growth of a hexagonal lyotropic phase (in French)*. PhD thesis, École Normale Supérieure de Lyon, 1996.

[68] L. Sallen, P. Sotta, and P. Oswald. Pretransitional effects near the hexagonal–micellar phase transition of the $C_{12}EO_6/H_2O$ lyotropic mixture. *J. Phys. Chem. B*, 101(25):4875–4881, 1997.

[69] V. Schmitt, F. Lequeux, A. Pousse, and D. Roux. Flow behavior and shear induced transition near an isotropic/nematic transition in equilibrium polymers. *Langmuir*, 10(3):955–961, 1994.

[70] W. Schnepp, S. Disch, and C. Schmidt. H^2 NMR–study on the lyomesophases of the system hexaethylene glycol dodecyl methyl-ether water – temperature-dependence of quadrupole splittings. *Liq. Cryst.*, 14(3):843–852, 1993.

[71] J. V. Selinger and R. F. Bruinsma. Hexagonal and nematic phases of chains. I. Correlation functions. *Phys. Rev. A*, 43(6):2910–2921, 1991.

[72] J. V. Selinger and R. F. Bruinsma. Hexagonal and nematic phases of chains. II. Phase transitions. *Phys. Rev. A*, 43(6):2922–2931, 1991.

[73] Y. A. Shchipunov and H. Hoffmann. Growth, branching, and local ordering of lecithin polymer-like micelles. *Langmuir*, 14(22):6350–6360, 1998.

[74] R. Strey. Water–nonionic surfactant systems, and the effect of additives. *Ber. Bunsen-Ges. Phys. Chem.*, 100(3):182–189, 1996.

[75] R. Strey, W. Jahn, G. Porte, and P. Bassereau. Freeze-fracture electron-microscopy of dilute lamellar and anomalous isotropic (L_3) phases. *Langmuir*, 6(11):1635–1639, 1990.

[76] R. Strey, W. Jahn, G. Porte, J. Marignan, and U. Olsson. Fluid membranes in the Water/NaCl-AOT system : A study combining small-angle neutron-scattering, electron microscopy and NMR self-diffusion. In S.-H. Chen, J. S. Huang, and P. Tartaglia, editors, *Structure and Dynamics of Strongly Interacting Colloids and Supramolecular Aggregates in Solution*, volume 369 of *NATO ASI Series, Series C : Mathematical and Physical Sciences*, pages 351–363. Kluwer, Dordrecht, 1992.

[77] I. Szleifer, D. Kramer, A. Ben-Shaul, D. Roux, and W. M. Gelbart. Curvature elasticity of pure and mixed surfactant films. *Phys. Rev. Lett.*, 60(19):1966–1969, 1988.

[78] P. Tolédano and A. M. Figueiredo Neto, editors. *Phase Transitions in Complex Fluids*. World Scientific, Singapore, 1998.

[79] K. J. Wiese. Polymerized membranes, a review. volume 19 of *Phase transitions and critical phenomena*. Academic Press, London, 2000.

[80] L. Yang and H. W. Huang. Observation of a membrane fusion intermediate structure. *Science*, 297(5588):1877–1879, 2002.

[81] J. Zimmerberg and L. V. Chernomordik. Membrane fusion. *Adv. Drug Deliv. Rev.*, 38(3):197–205, 1999.

[82] M. Zulauf, K. Weckström, J. Hayter, V. Degiorgio, and M. Corti. Neutron scattering study of micelle structure in isotropic aqueous solutions of poly(oxyethylene) amphiphiles. *J. Phys. Chem.*, 89(15):3411–3417, 1985.